Cell Communication
and Signaling

RESEARCH

ASIC3-activated key enzymes of *de novo* lipid synthesis supports lactate-driven EMT and the metastasis of colorectal cancer cells

Xing Wan[1,2], Feng Li[1], Zhigui Li[3] and Liming Zhou[1,2]*

Abstract

Acidic microenvironments is a cancer progression driver, unclear core mechanism hinders the discovery of new diagnostic or therapeutic targets. ASIC3 is an extracellular proton sensor and acid-sensitive, but its role in acidic tumor microenvironment of colorectal cancer is not reported. Functional analysis data show that colorectal cancer cells respond to specific concentration of lactate to accelerate invasion and metastasis, and ASIC3 is the main actor in this process. Mechanism reveal *de novo* lipid synthesis is a regulatory process of ASIC3, down-regulated ASIC3 increases and interacts with ACC1 and SCD1, which are key enzymes in *de novo* lipid synthesis pathway, this interaction results in increased unsaturated fatty acids, which in turn induce EMT to promote metastasis, and overexpression of ASIC3 reduces acidic TME-enhanced colorectal cancer metastasis. Clinical samples of colorectal cancer also exhibit decreased ASIC3 expression, and low ASIC3 expression is associated with metastasis and stage of colorectal cancer. This study is the first to identify the role of the ASIC3-ACC1/SCD1 axis in acid-enhanced colorectal cancer metastasis. The expression pattern of ASIC3 in colorectal cancer differs significantly from that in other types of cancers, ASIC3 may serve as a novel and reliable marker for acidic microenvironmental in colorectal cancer, and potentially a therapeutic target.

Keywords Colorectal cancer, Acidic tumor microenvironment, ASIC3, *De novo* lipid synthesis, EMT, Metastasis

Background

Cancer is a complex and polymorphic disease, with its surrounding environment being a key factor that sets it apart from normal tissues and influences cancer progression and behavior. This environment, known as the tumor microenvironment (TME), is characterized by various features. While hypoxia is extensively studied [1], acidity is another prevalent yet less explored characteristic. Tumor tissues often exhibit a pH of 6.6 or lower [2].

Although not as extensively studied as hypoxia, an increasing number of studies have focused on the effect of acidic TME on tumor phenotypes. Recent research indicates that the acidic TME significantly influences carcinogenesis by modulating various aspects of cancer behavior [3], such as proliferation [4], invasion [5], *metastasis* [6], stemness, and cell death [7]. Nevertheless, the clinical efficacy of acidosis-targeted treatments varies depending on the cancer type, pathological stage and metastatic phase. A mere 0.1 unit change in the intracellular and extracellular pH ratio can trigger biological or pathological effects [8]. These findings suggest that acidity-mediated tumor response are organ - or cancer-specific.
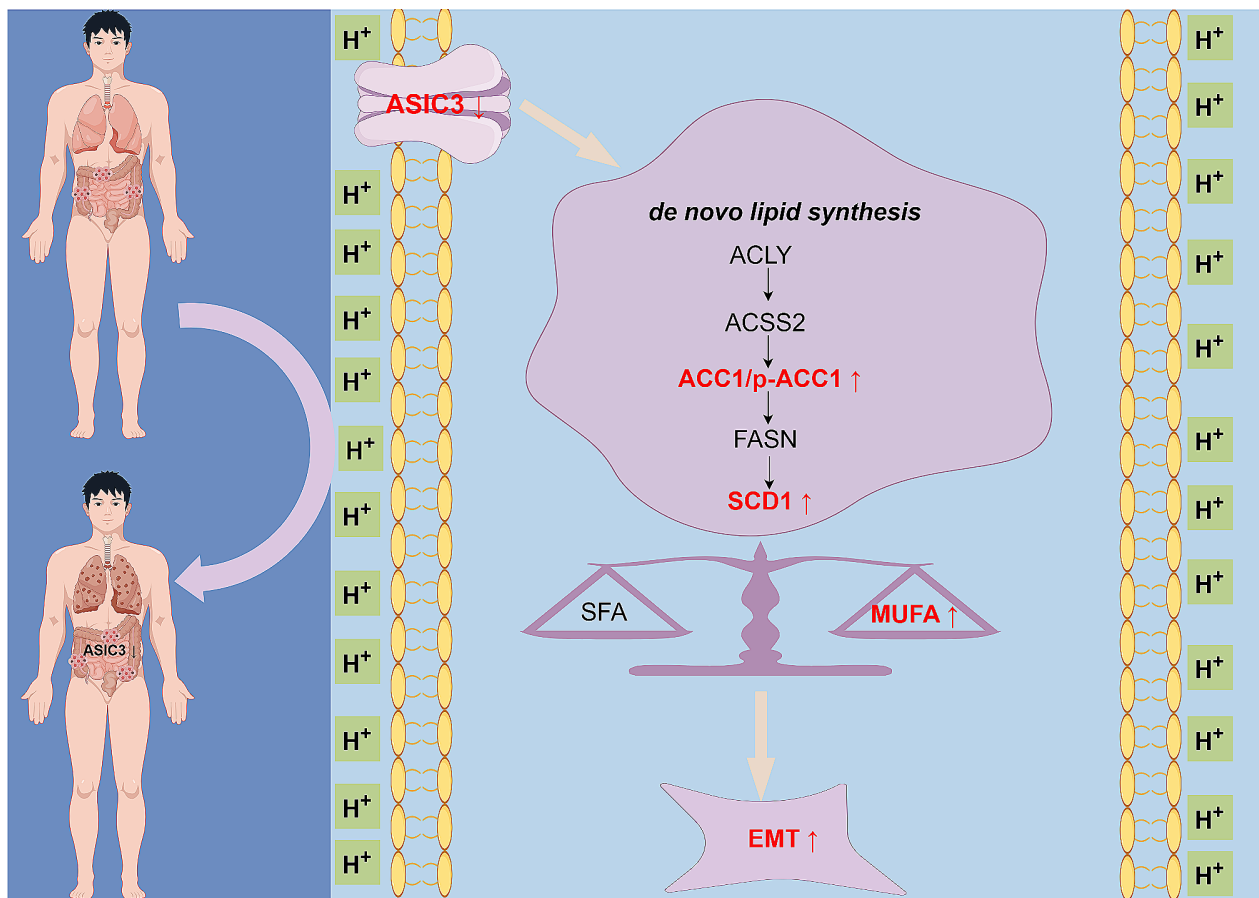
*Correspondence:
Liming Zhou
zhoulim@scu.edu.cn
Full list of author information is available at the end of the article

Graphical Abstract

In addition, although acidosis is associated with many behaviors in cancer cells, such as inducing autophagy [9], regulating immune responses [10], or inducing EMT to lead to metastasis, most of these factors are localized in organelles or cytoplasm, so how do they actually sense changes in extracellular pH? Extracellular proton sensors, such as G-protein-coupled receptors and receptor protein tyrosine phosphatase-γ, are particularly important in detecting extracellular pH changes [11]. Another set of sensors, including acid-sensitive ion channels(ASICs), are currently less studied, but are potentially significant due to their sensitivity to acid, warranting further investigation in solid tumors.

Tumor biopsies show that lactate levels in invasive colorectal cancers(CRC) are almost 2–4 times higher than that in non-invasive ones [12], suggesting a role for the acidic microenvironment in CRC metastasis. Our current study demonstrates that a specific concentration of lactate stimulating cells for a certain period of time can lead to a notable decrease and desensitization of ASIC3, therefore, ASIC3 may be a reliable biomarker for colorectal cancer acidosis, as its decrease correlates with cancer differentiation, stage, and metastasis. Furthermore, our investigation into the downstream signals mediated by ASIC3 reveals a connection between extracellular protons and intracellular signaling pathways, enhancing our understanding of acidosis's impact on colorectal cancer metastasis. Metabolic reprogramming is an important cancer marker, with the identification of ASIC3-ACC1/ SCD1-MUFA axis in colorectal cancer cells, the mechanism by which ASIC3 modulates the *de novo* lipid synthesis pathway provides a foundation for utilizing ASIC3 in the diagnosis and treatment of colorectal cancer.

Methods

Materials

All consumables, reagents, cells and animal information are provided in supplement Tables 1, 2 and 3.

Wan *et al. Cell Communication and Signaling*   (2024) 22:388

Page 3 of 17

Clinical samples

The 245 cases of primary CRC tissues and adjacent tissues were collected at the West China Hospital, Sichuan University between 2019 and 2021 year. The collection and use of human tissues for this study were approved by the Ethics Committee of West China Hospital. Written informed consent was obtained from patients before sampling.

Cell culture

HCT116, SW480, CCD841CoN, HT29, HT15, RKO, DLD1, SW620 and HuH-7 cells were cultured in Dulbecco's Modified Eagle's Medium (DMEM) medium supplemented with 10% fetal bovine serum (FBS) and 1% penicillin/streptomycin, incubated in a 5% CO2 humidified incubator at 37℃.

Western blot

The gel was electrophoretic at 110v using SDS-PAGE with different concentrations according to the molecular weight of the protein. Then according to the molecular weight, choose different transfer time with constant pressure 110v. Band was closed with 5% skim milk powder for 1 h, incubated with the primary antibody overnight(see supplement Table 4 for protein information and antibody ratios), washed with TBST for three times for 10 min each time, incubated with the secondary antibody at room temperature for 90 min, washed with TBST for three times, and exposed on the developer.

CCK8

The cells were inoculated to 96-well plates with a density of about 70%. On the next day, the medium was discarded and serum-free medium with different concentrations of lactate was added, and incubated 24/48/72 h. After reaching the point, the 96-well plate was taken out, the medium was discarded, and the medium containing cck8 was added and incubated for 30 min with 100ul per well. Absorbance was measured at 450 nm.

Scratch test

The cells were inoculated to 24 well plates. When the cells were gathered to 100%, a vertical line was drawn in the middle of the hole plate with a 200ul suction head along a ruler, the medium was discarded, cleaned twice with PBS, and the medium with different concentrations of lactic acid but without serum was added, and photos were taken. After 24 h/48 h/72 h, the photo was taken again at the same position.

Transwell assay

Dilute the matrigel at 1:20, give 80ul matrigel to each chamber, and put the well plate in the incubator for 3 h. Add 600ul DMEM containing 10%FBS in lower chamber, digest the cells, add 100ul of cell suspension in the upper chamber and supplement to 200ul with serum-free medium. Ensure that the cells in each well are same, usually is $4 \sim 8 \times 10^4$ according to cell types. For the group that needs to add lactate, add it in both upper and lower chambers. Cells were fixed with paraformaldehyde for 30 min, dyed with 0.1% crystal violet for 30 min, washed with PBS to remove floating color, dried, and photographed.

Lung metastasis model in nude mice

4 week-old nude mice were adaptively fed for one week. The cells were cultured with lactate for 1 day and then injected into the animals through the tail vein. Each animal was given 0.2mL and the cells were 1.5×10^6.The same operation is suitable for overexpressed stable transmutation. After 6 weeks of feeding, after gas anesthesia, blood was taken from the eyeballs, and then the nude mice were killed and lungs were taken. All animal experiments meet the requirements of Animal Ethics Committee of Sichuan University.

HE staining

Lung samples were fixed in 10% formaldehyde. Tissues were washed with tap water, dehydrated in alcohol and embedded in paraffin. Staining were performed with HE stain. Results were recorded by panoramic scanning with panoramic MIDI and scanned with Case Viewer2.4 software.

Bioanalysis

All bioinformatics analysis is done on three websites: GEPIA (gepia.cancer-pku.cn), ACLBI(www.aclbi.com) and the human protein atlas(www.proteinatlas.org).

Real time PCR

Expression of target gene and GAPDH were measured after extraction of RNA, total RNA was reversely transcribed using PrimeScriptR RT Master, quantitative PCR was carried out with SYBR Premix Ex Taq™ II in ABI QuantStudio3 in accordance with kit instruction, data analysis was performed using the $2^{-\Delta\Delta CT}$ method for relative quantification, all of the gene expression levels were calculated relative to the GAPDH. Primers are synthesized at BGI, see Supplement Table 5.

shRNA transfection

When the cells converged to 70%, 7.5μL lip3000 was first diluted with 125μL opti-DMEM, then 2.5 μg shRNA plasmid and 5μL P3000 were diluted with 125μL opti-DMEM, the two were mixed, incubated at room temperature for 15 min, and 250μL complex was added to one hole of the 6-well plate. Target Seq of sh1 is GCCCTCC CTATACCCTTAT. Target Seq of sh2 is GCTGCCGAAT

GGTGTACAT. Target Seq of sh3 is CCCTGGACATCTT CTTTGA.

Lentivirus infection

ASIC3 vector titer is 2×10^8TU/mL, negative vector titer is 8×10^8TU/mL. According to the preliminary experiment, the appropriate infection condition MOI=10 was obtained. Virus volume=20×cell number/titer(µL). Polybrene was diluted 200 times to aid infection. Infection complex was composed of 100 polybrene, virus and DMEM. Added this 1mL complex to 6-well plate, screened positive cells with puromycin for one week to obtain stable transmutation strains. Primer sequence: XhoI: CTACCGGACTCAGATCTCGAGGCCACCATG AAGCCCACCTCAGGCCCAG,

   NotI: GGTCTTTGTAGTCGCGGCCGCGGAGCTGT GTGACAAGGTAGCAGGTG.

Immunohistochemistry

After embedded in paraffin, lung tissues were repaired for 90s in high temperature and high pressure, incubated with blocking solution (10% goat serum) at room temperature for 30 min, then incubated with primary antibodies (ASIC3 1:400) overnight at 4 °C, after that, 50 µL appropriate secondary antibodies for each slide were added and incubated for 45 min at 37°. After conventional treatment, slides were checked by panoramic scanning with panoramic MIDI.

Oil red staining

Remove the 6-well plate, discard the medium, and clean it with PBS. After two times of cleaning, add 1mLof paraformaldehyde to fix it for 30 min. Discard the paraformaldehyde, cover it with dyeing solution for 30s, discard the dyeing solution, add oil red dyeing solution, and incubation for 15 min away from light. Take pictures directly or do it after washing them with pbs.

LC-MS

1×10^7 cells were collected and quenched with liquid nitrogen. Transferred cell samples into a 2 mL centrifuge tube, added 100 mg glass beads, and then accurately added 750 µL of mixed solvent (chloroform : methanol, 2:1, v/v) at -20 ℃, and vortexed for 30 s; the sample was rapidly frozen in liquid nitrogen for 5 min, then frozen and thawed at room temperature, and vortexed for 2 min at 50 Hz; Left the tube to ice for 40 min, added 190 µL H_2O, vortexed for 30 s, and still incubated ice for 10 min; centrifuged at 12,000 rpm for 5 min at room temperature and transferred 300 µL organic layer into a new centrifuge tube; added 500 µL of mixed solvent (chloroform : methanol, 2:1, v/v), vortexed for 30 s; centrifuged at 12,000 rpm for 5 min at room temperature and transfer 400 µL organic layer into the same centrifuge tube.

Samples were concentrated to dry in vacuum; dissolved samples with 200 µL isopropanol, and the supernatant was filtered through 0.22 µm membrane to obtain the prepared samples for LC-MS. The instrument operation is completed in Suzhou PANOMIX Biomedical Tech Co., LTD.

CO-IP

The cells were cultured in a 10 cm petri dish, and when the cells were fully confluent, 180 µl NP40 lysate was added to each cell, and the cells were scraped off, cleaved on ice for 30 min, and swirled every 5 min. The cells were divided into three equal parts, each 125µL, and the first part was denatured with loading buffer as input group. Added 2ug of IgG and ASIC3 primary antibody to the remaining two, added 40 µL magnetic beads per tube. Incubated on ice for 8 h. Removed the supernatant by absorbing the magnetic beads with a magnetic rack, washed with 1mL lysate for 4 times, and finally added 30µL loading buffer to denature. The magnetic rack absorbed the magnetic beads and left the supernatant for WB.

Statistical analysis

The results were presented with Mean±SD and analyzed using GraphPad Prism10.0. Unpaired/paired T-test was applied to analyze two sets of data, the association between ASIC3 expression and pathological features was analyzed using the chi-squared test and Fisher's exact test. while one-way ANOVA followed by a post hoc Dunnett-t-test to perform multiple comparisons. For statistical significance, *or[#], **or [##], and *** denote *P* value of <0.05, 0.01, 0.001 respectively.

Results

ASIC3 was down-regulated in colorectal cancer

To assess the significance of the target gene ASIC3, we initially examined its expression profile in pan-cancer in the TCGA database. Our findings revealed that ASIC3 is prevalent in most tumors and is typically down-regulated (Fig. 1A). Subsequently, utilizing the GEPIA website, we investigated ASIC3 expression in colorectal cancer, confirming a down-regulation of ASIC3 mRNA (Fig. 1B). Additionally, analysis of colon cancer and rectal cancer tissues from the human protein atlas website indicated negative expression of ASIC3 (Fig. 1C). Despite reports of increased ASIC3 levels in lung cancer, pancreatic cancer, bone cancer, and glioblastoma [13–16], our study focused on colorectal cancer. We conducted a clinical study involving 245 pairs of colorectal cancer tissues from West China Hospital. Our results demonstrated a significant down-regulation of ASIC3 mRNA in colorectal cancer tissues compared to adjacent tissues, with a high rate of low expression (170/245, approximately
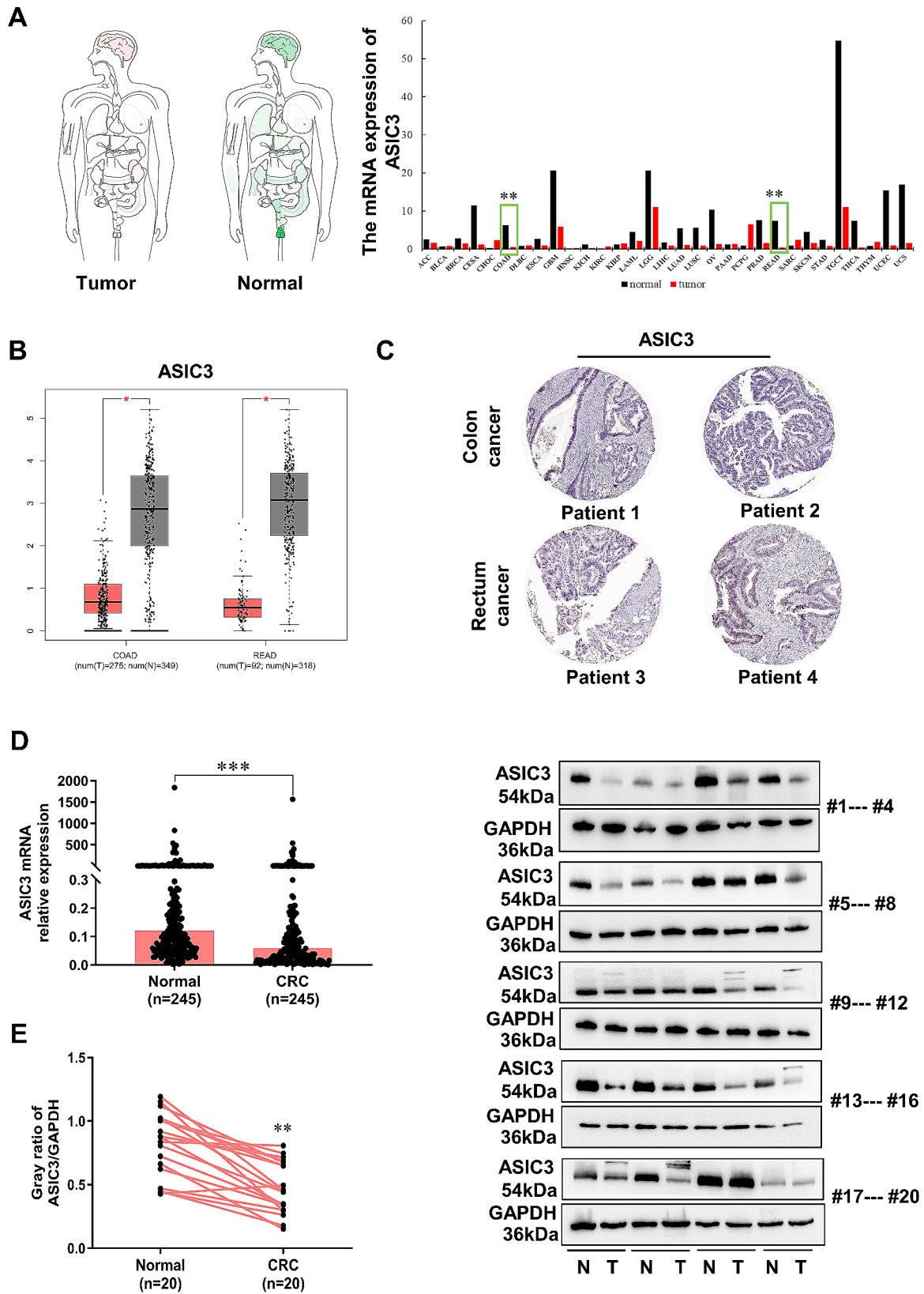
Fig. 1 ASIC3 was down-regulated in colorectal cancer. **A** The expression of ASIC3 in different tumors from TCGA database. **B** The expression of ASIC3 in colorectal cancer from TCGA database. **C** The expression of ASIC3 by IHC in colon and rectum cancer patients. **D** The mRNA expression of ASIC3 tested by QPCR in 245 CRC patients. **E** The protein expression of ASIC3 tested by WB in 20 CRC patients and its gray ratio. Error bars represent SD, $**p < 0.01$, $***p < 0.001$
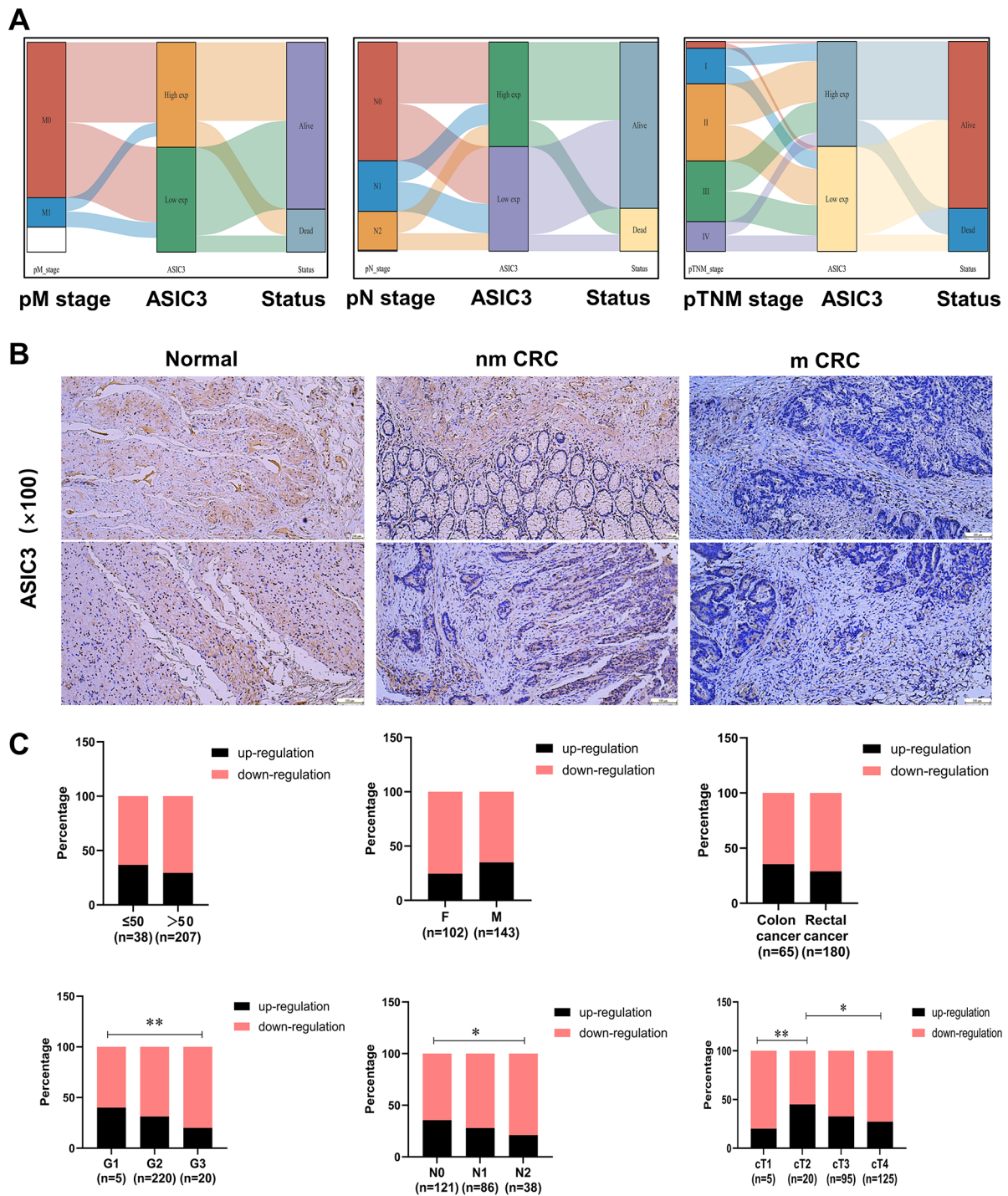
Fig. 2 Downregulation of ASIC3 is associated with clinical stage and metastasis. **A** The relationship between ASIC3 expression and distal metastasis, lymphatic metastasis and clinical staging by bioanalysis. **B** The expression of ASIC3 tested by IHC in normal tissue and CRC patients with non-metastasis and metastasis. **C** The relationship between ASIC3 mRNA and clinical features. Error bars represent SD, *$p < 0.05$, **$p < 0.01$

69.4%) (Fig. 1D). Furthermore, Western blot analysis of ASIC3 protein expression in tissues from 20 colorectal cancer patients also revealed lower levels in cancerous tissues compared to adjacent tissues (Fig. 1E). These findings underscore the distinct expression pattern of ASIC3 in colorectal cancer compared to other cancer types.
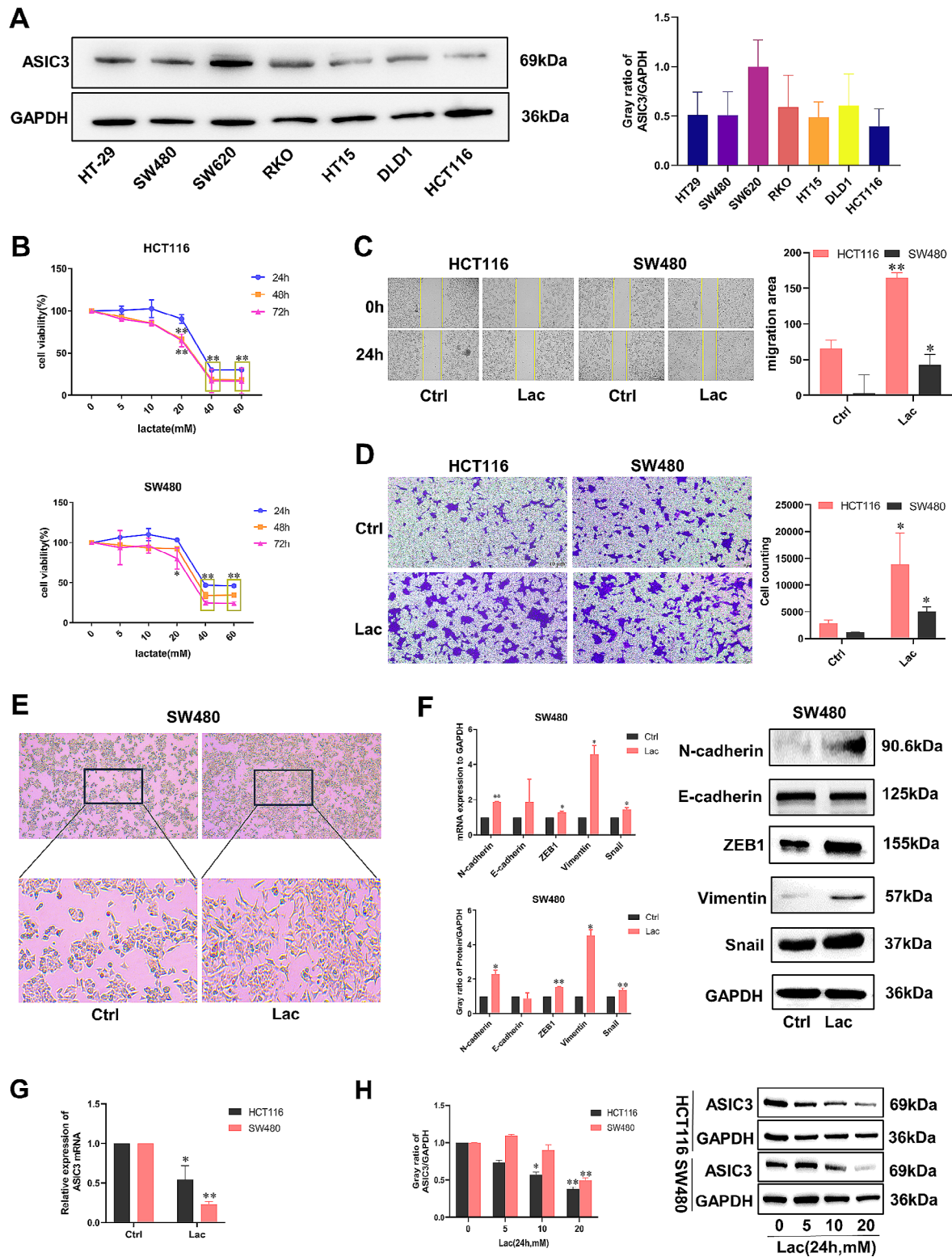
Fig. 3 Lactate downregulates ASIC3 and induces EMT to promote migration and invasion. **A** The protein expression of ASIC3 in different colorectal cancer cells and its gray ratio. **B** cell viability affected by lactate tested by CCK8 in HCT116 and SW480 cells. **C** The effect of lactate on CRC cell migration detected by scratch test at 24 h and Migration area statistics in HCT116 and SW480 cells. **D** The effect of lactate on CRC cell invasion detected by Transwell and invasion cell statistics HCT116 and SW480 cells. **E** The morphologic change of SW480 treated without and with lactate. **F** The effect of lactate on EMT markers in SW480 cell tested by QPCR, WB and its gray ratio. **G** and **H** The effect of lactate on ASIC3 mRNA and protein expression by QPCR and WB at lactate stimulating for 24 h in HCT116 and SW480 cells. Error bars represent SD, *$p < 0.05$, **$p < 0.01$
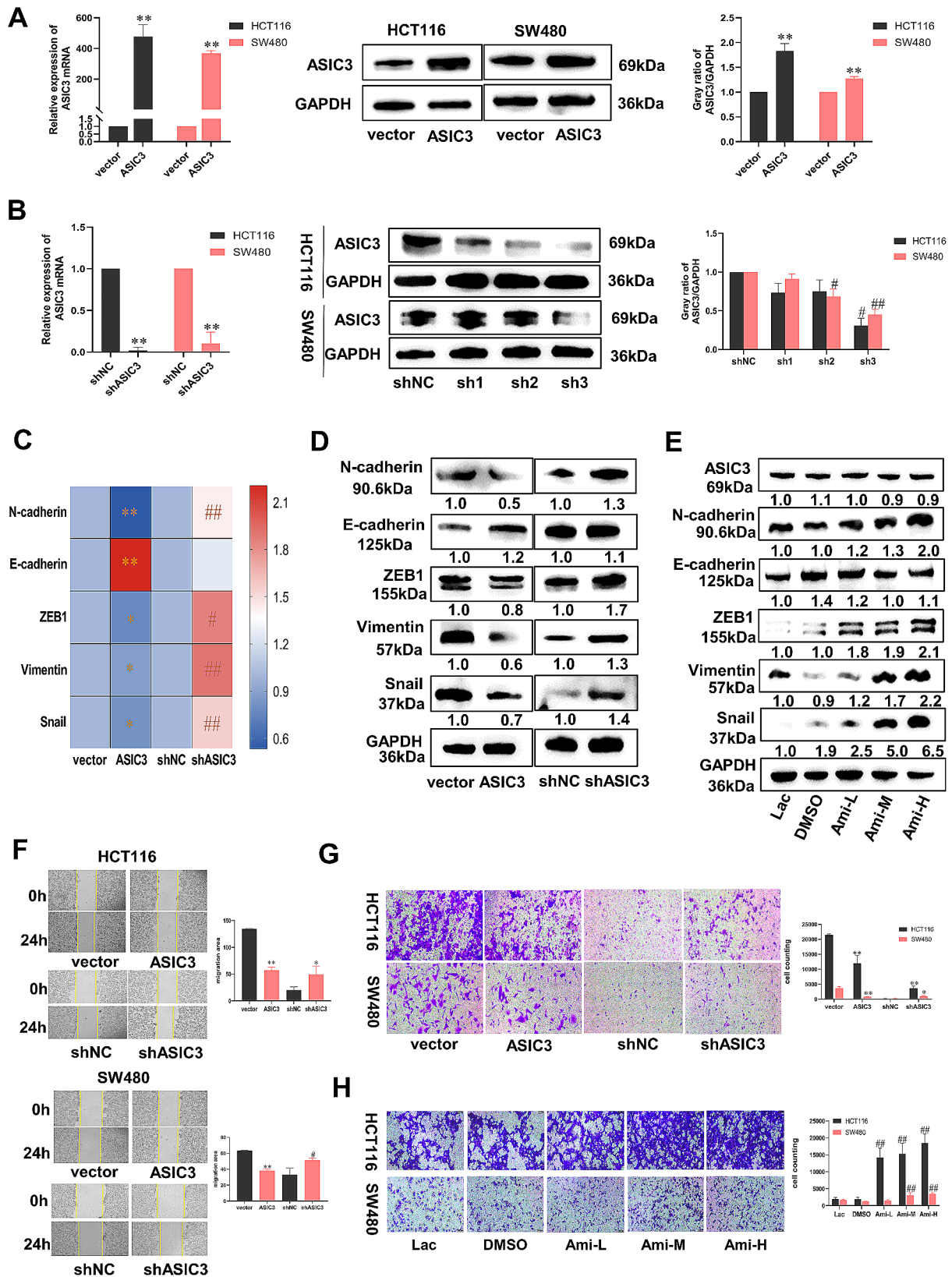
Fig. 4 (See legend on next page.)

(See figure on previous page.)

Fig. 4 ASIC3 is down-regulated under lactate stimulation to induce EMT and invasion. **A** and **B** The effect of lactate on ASIC3 mRNA and protein expression by QPCR and WB at lactate stimulating for 24 h in HCT116 and SW480 cells. **A** The mRNA expression tested by QPCR and protein expression tested by WB of ASIC3 when ASIC3 overexpressed by lentivirus in HCT116 and SW480 cells. **B** The mRNA expression tested by QPCR and protein expression tested by WB of ASIC3 when ASIC3 knocked down by shRNA in HCT116 and SW480 cells. **C** and **D** The expression of EMT markers tested by QPCR and WB when ASIC3 overexpressed by lentivirus and knocked down by shRNA in HCT116 cell. **E** The expression of EMT markers tested by WB when ASIC3 channel blocked by inhibitor Amiloride in HCT116 cell. **F** and **G** The migration and invasion change when ASIC3 overexpressed by lentivirus and knocked down by shRNA in HCT116 and SW480 cells. **H** The invasion change when ASIC3 channel blocked by inhibitor Amiloride in HCT116 and SW480 cells. Error bars represent SD, *or $^{\#}p < 0.05$, **or $^{\#\#}p < 0.01$

Downregulation of ASIC3 is associated with clinical stage and metastasis

To assess the clinical significance of ASIC3 in CRC, we initially conducted a biogenic analysis which revealed its association with distal metastasis, lymphatic metastasis, and clinical stage (Fig. 2A). Subsequently, we used IHC to detect ASIC3 expression in normal intestinal tissue, non-metastatic and metastatic colorectal cancer, revealing lower ASIC3 expression in metastatic colorectal cancer sites (Fig. 2B). Lastly, according to the results of ASIC3 mRNA expression obtained from 245 pairs of patients, the relationship between ASIC3 mRNA and clinical characteristics was analyzed, and it was found that ASIC3 was indeed correlated with tumor differentiation, lymphatic metastasis and clinical stage(Fig. 2C).

Lactate downregulates ASIC3 and induces EMT to promote migration and invasion

Tumor acidic microenvironment, a prominent characteristic of tumors, is primarily induced by factors such as fibroblast secretion and lactic acid generated from aerobic glycolysis. In this study, we opted for a common approach to replicate the extracellular acidic conditions using a medium containing lactate [17, 18]. Given the down-regulation of ASIC3 in clinical samples, our investigation focused on HCT116 colon cancer cells and SW480 rectal cancer cells, both exhibiting reduced ASIC3 expression(Fig. 3A). Varying levels of lactate are present in different cancer tissues, prompting us to assess the impact of different lactate concentrations on cell viability and migration ability using CCK8 and scratch tests at 24 h, 48 h, and 72 h. Results revealed that treatment with 20mM lactate for 24 h was advantageous for CRC, displaying no cytotoxic effects but significantly enhancing cell migration capacity(Fig. 3B-C; Fig. S3A). Additionally, Transwell assays demonstrated a marked increase in invasive cell numbers with 20mM lactate treatment(Fig. 3D). EMT is a marker for invasion, further evaluation of cell morphology and EMT markers in lactate-treated cells revealed irregular spindle transformations (Fig. 3E; S3B) and elevated expression of EMT-related genes (N-cadherin, ZEB1, Vimentin, and Snail) at both mRNA and protein levels, while E-cadherin levels remained relatively unchanged(Fig. 3F; S3C). ASIC3 is an acid receptor. *Subsequent analysis of ASIC3 expression in an acidic tumor microenvironment post lactate stimulation indicated a reduction in ASIC3 mRNA and protein levels in a time- and dose-dependent manner*(Fig. 3G-H; Figure S3D), suggesting a consistent downregulation of ASIC3 under prolonged lactate exposure.

ASIC3 is a key factor in lactate induced EMT, migration and invasion

We used lentivirus and shRNA to overexpress and knock down ASIC3 respectively to know the effect of ASIC3 under acidic tumor microenvironment. QPCR and WB experiments were used to verify the interference effect(Fig. 4A-B). Our study explored the influence of ASIC3 on the mRNA and protein expression of EMT markers ,as well as its effects on cell morphology. Results indicated that under acidic conditions, knocking down ASIC3 led to increased expression of EMT-related genes at both mRNA and protein levels, along with a higher number of fusiform cells and enhanced interstitial cell formation. Conversely, overexpression of ASIC3 yielded opposite outcomes (Fig. 4C-D; Figure S4A-C); in order to explain the regulation of EMT by ASIC3 from multiple perspectives, we also used Amiloride here, an inhibitor of ASIC3 ion channel, and found that after the closure of ASIC3 channel, the expression of EMT-related proteins was also stimulated(Fig. 4E; Figure S4D). Subsequent experiments involving Scratch tests and Transwell assays demonstrated that ASIC3 influenced CRC migration and invasion in an acidic microenvironment, with overexpression reducing migration and invasion, while knockdown increased these processes (Fig. 4F-G). Furthermore, administration of Amiloride resulted in a dose-dependent increase in the number of invasive cells (Fig. 4H).

Down-regulation of ASIC3 can activate key enzymes of *de novo* lipid synthesis and increase the content of MUFA

Lipid reprogramming is a carcinogenic marker, paper elucidated that SCD1 regulates EMT in colorectal cancer [19], even one paper revealed that tumor microenvironment acidity can trigger lipid accumulation in liver cancer via SCD1 [17]. Stearoyl-coenzyme A desaturase-1 (SCD1), a crucial enzyme in *de novo* lipid synthesis, functions as a fatty acyl Δ-9 desaturase, converting saturated fatty acids (SFAs) like palmitic acid (C16:0FA) to monounsaturated fatty acids
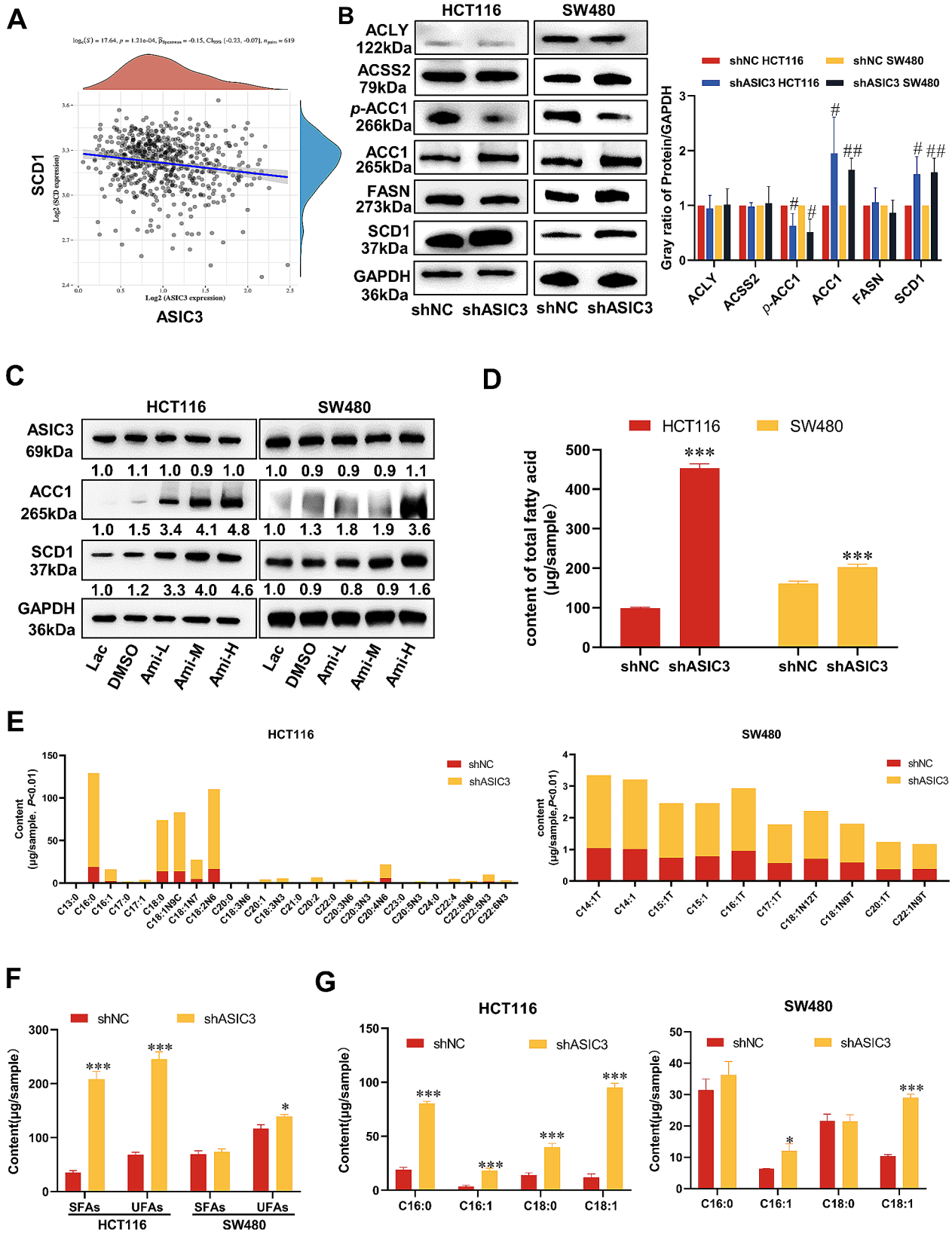
Fig. 5 (See legend on next page.)

(See figure on previous page.)

Fig. 5 Down-regulation of ASIC3 can activate key enzymes of *de novo* lipid synthesis and increase the content of MUFA. **A** The relationship between ASIC3 and SCD1 in TCGA database from GEPIA website. **B** The protein expression of *de novo* lipid synthesis key enzymes and ACSS2 tested by WB when ASIC3 was knocked down by shRNA in HCT116 and SW480 cells under acidic condition and their gray ratio statistics. **C** The protein expression of ACC1 and SCD1 tested by WB when ASIC3 channel blocked by inhibitor Amiloride and their gray ratio statistics in HCT116 and SW480 cells. **D** The content change of total fatty acids when ASIC3 knocked down under lactate stimulation in HCT116 and SW480 cells. **E** The different kinds of fatty acids which increased when ASIC3 knocked down under lactate stimulation in HCT116 and SW480 cells. **F** The content change of saturated and unsaturated fatty acids when ASIC3 knocked down under lactate stimulation. **G** The content change of saturated and monounsaturated C16 and C18 fatty acids when ASIC3 knocked down under lactate stimulation. Error bars represent SD, *or $^{\#}p < 0.05$, $^{\#\#}p < 0.01$, ***$p < 0.01$

(MUFAs) such as palmitoleic acid (C16:1FA), or stearic acid (C18:0FA) to oleic acid (C18:1FA) [20–21], so we identified its expression by bioanalysis and in clinical samples, it indeed increased in CRC. Interestingly, we observed a negative correlation between SCD1 and ASIC3 with bioanalysis (Fig. 5A; Figure S5A-C). But the *de novo* lipid synthesis pathway involves a range of enzymes, in studying the mechanism mediated by ASIC3 in the acidic tumor microenvironment, we were curious whether these enzymes besides SCD1 were regulated. According to the source of acetyl-CoA, the key enzymes to produce unsaturated fatty acids include: ACLY, ACSS2, ACC1/p-ACC1, FASN, SCD1, we found that knocking down ASIC3 increased the expression of ACC1/p-ACC1 and SCD1 while other enzymes did not change(Fig. 5B). Blocking ASIC3 channel could also increase these two enzymes(Fig. 5C). This upregulation of key enzymes in the *de novo* lipid synthesis pathway upon ASIC3 knockdown prompted us to examine if there were alterations in the fatty acid products. Our GC-MS results show reducing ASIC3 led to an overall increase in total fatty acid content (Fig. 5D), with saturated fatty acids (SFA) and unsaturated fatty acids (UFA) increasing in HCT116 cells, and monounsaturated fatty acids (MUFA) also rising in SW480 cells (Fig. 5E-F). Meanwhile, the changes of classical fatty acids C16 and C18 were analyzed, we observed significant increases in both saturated and unsaturated C16 and C18 fatty acids in HCT116, while MUFA levels of C16 and C18 showed a notable increase in SW480 (Fig. 5G).

Increased MUFA in acidic microenvironment can induce EMT

Under lactate stimulation, knockdown of ASIC3 leads to an increase in the key enzyme of *de novo* lipid synthesis and its product MUFA. Therefore, we examined the changes of MUFA and different types of lipids during lactate stimulation and elucidated their effects on lactate-induced EMT. In average, 343 kinds of lipids were changed, with 260 lipids showing an increase in the lactate group (Fig. 6A), among these, the TG category exhibited the most significant increase in lipid numbers (Fig. 6B), the relative expression of total TG in control group and lactate group was calculated, and lactate did increase the content of total TG(Fig. 6C), meanwhile, we

detected the lipid content of different double bonds in TG types, and found that unsaturated fatty acids containing one double bond increased most obviously(Fig. 6D), so we listed the two most obvious TG containing one double bond(Fig. 6E), to further illustrate lipid changes, we detected lipid droplet aggregation using oil red O staining and found that lactate increased lipid droplet accumulation(Fig. 6F). Specifically, Palmitodiolein (TG), oleic acid (OA): a C18:1 monounsaturated fatty acid, and a C16:1 palmitoleic acid (POA) were selected to confirm that products and derivatives of*de novo* lipid synthesis could enhance lipid droplet accumulation (Fig. 6G) and induce EMT (Fig. 6H).

Inhibition of ACC1 and SCD1 reverses the function of ASIC3 in the acidic tumor microenvironment

The relationship between key enzymes in *de novo* lipid synthesis and phenotype was further clarified due to interference with ASIC3 affecting ACC1 and SCD1, leading to product changes. We found that inhibiting ACC1 and SCD1 can inhibit EMT and invasion(Fig. 7A-B; Figure S7A). Through recovery experiments, we were able to demonstrate that ASIC3 influences EMT and invasion via ACC1 and SCD1 (Fig. 7C-D; Figure S7B-C). Subsequently, CO-IP experiments were used to reveal the interaction between ASIC3 and ACC1 and SCD1 under lactate stimulation(Fig. 7E). Furthermore, inhibitor tests confirmed that ASIC3 acts upstream of ACC1 and SCD1 without any regulatory loop between the two (Fig. 7F; Figure S7D).
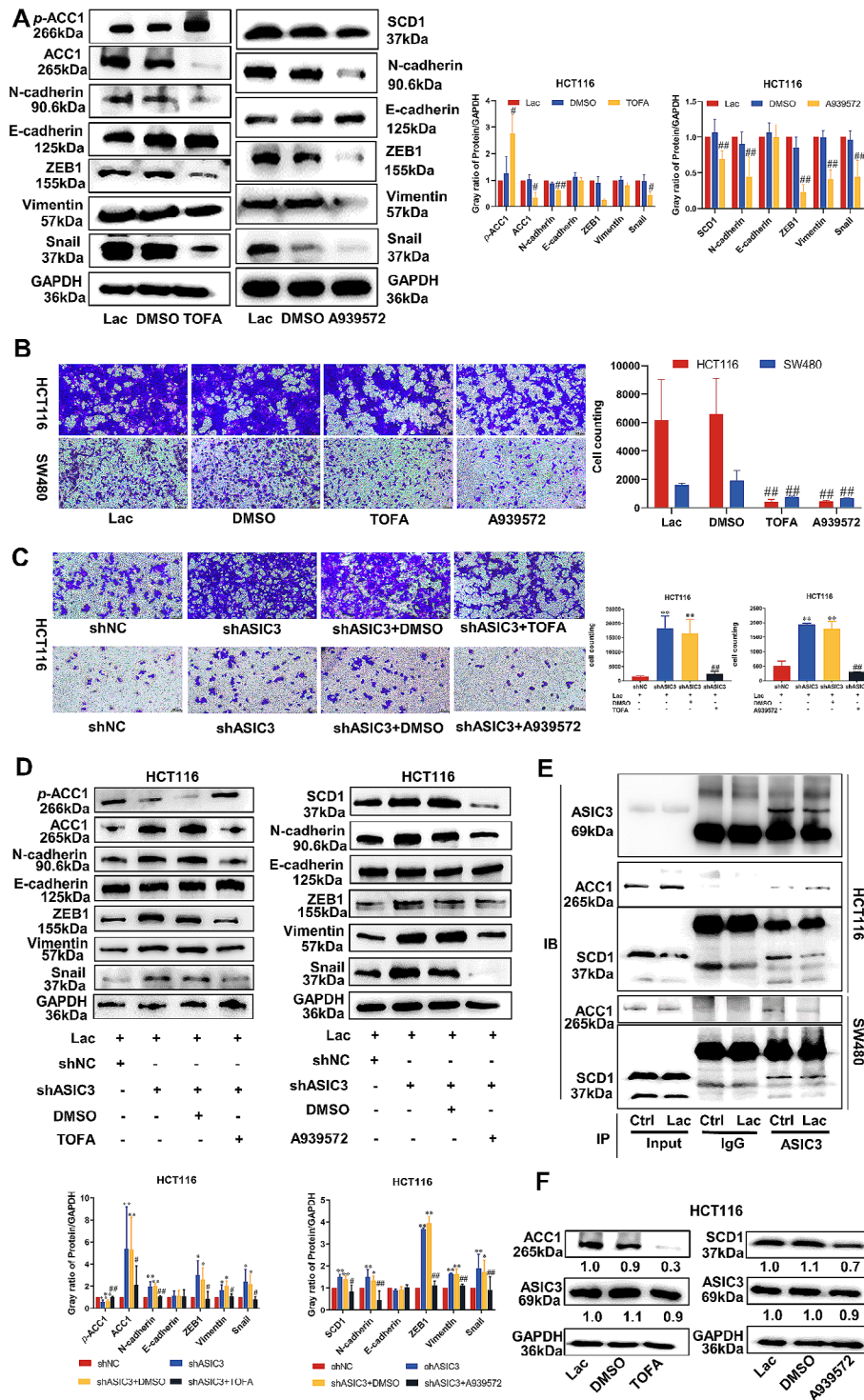
Overexpression of ASIC3 reverses lactate-induced lung metastasis

To investigate the impact of the acidic tumor microenvironment on metastasis, lactate-cultured HCT116 and SW480 cells were injected into the tail vein of nude mice. After 6 weeks, comparisons were made based on body weight, animal appearance, lung appearance, and HE staining for detecting colorectal cancer metastasis in the lungs. The experimental results showed that the colorectal cancer cells treated with lactate reduced the body weight of the animals compared to the untreated group(Fig. 8A). Additionally, lungs exhibited signs of scattered bleeding, swelling, and small particles on the surface (Fig. 8B), with HE staining revealing increased colorectal cancer cell metastasis in the lungs (Fig. 8C).
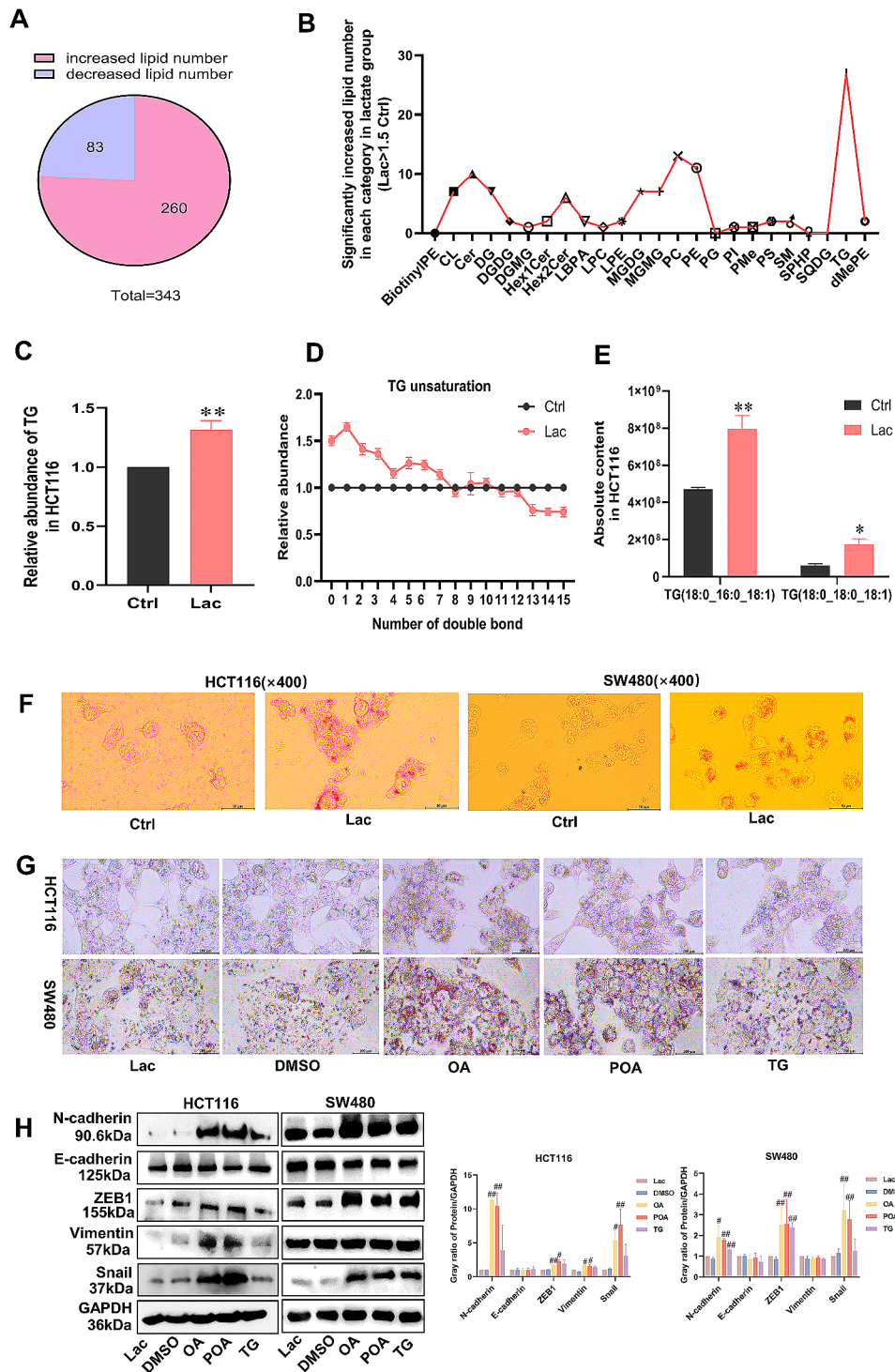
Fig. 6 Increased MUFA in acidic microenvironment can induce EMT. **A** The number of increased lipids and the number of decreased lipids when HCT116 cell cultured with lactate. **B** The number of significantly increased in different types of lipids when HCT116 cell cultured with lactate. **C** The effect of lactate on TG content in HCT116 cell tested by LC-MS. **D** The changes of TG containing different double bonds under lactate stimulation in HCT116 by LC-MS. **E** Two types of TG significantly increased under lactate stimulation in HCT116 cell. **F** The effect of lactate on lipid droplets of HCT116 and SW480 cells by Oil Red staining. **G** The effect of OA, POA, TG on lipid droplets under lactate stimulation tested by Oil Red staining in HCT116 and SW480 cells. **H** The effect of OA, POA, TG on the expression of EMT markers under lactate stimulation tested by WB in HCT116 and SW480 cells. Error bars represent SD, *or #$p < 0.05$, **or ##$p < 0.01$

Subsequent overexpression of ASIC3 in lactate-cultured   cells reversed the effects of lactate, resulting in weight

Fig. 7 Inhibition of ACC1 and SCD1 reverses the function of ASIC3 in the acidic tumor microenvironment. **A** The expression of EMT markers affected by ACC1 inhibitor and SCD1 inhibitor under lactate condition tested by WB and their gray ratio statistics. **B** The change of invasion cells affected by ACC1 inhibitor and SCD1 inhibitor under lactate condition in HCT116 and SW480 cells and their statistics. **C** The invasion cell change affected by ACC1 and SCD1 inhibitors on the basis of ASIC3 knocked down under acidic condition and invasion cell statistics. **D** The protein expression of EMT markers affected by ACC1 and SCD1 inhibitors on the basis of ASIC3 knocked down under acidic condition tested by WB and their gray ratio statistics. **E** The interaction effect of ASIC3 and ACC1,SCD1 by CO-IP, the ASIC3 primary antibody used as bait for IP experiment, and the expression of ASIC3,ACC1 and SCD1 detected by WB. **F** The protein expression of ASIC3 affected by ACC1 and SCD1 inhibitors tested by WB under acidic condition and their gray ratio statistics in HCT116 cell. Error bars represent SD, *or $^{\#}p < 0.05$, **or $^{\#\#}p < 0.01$
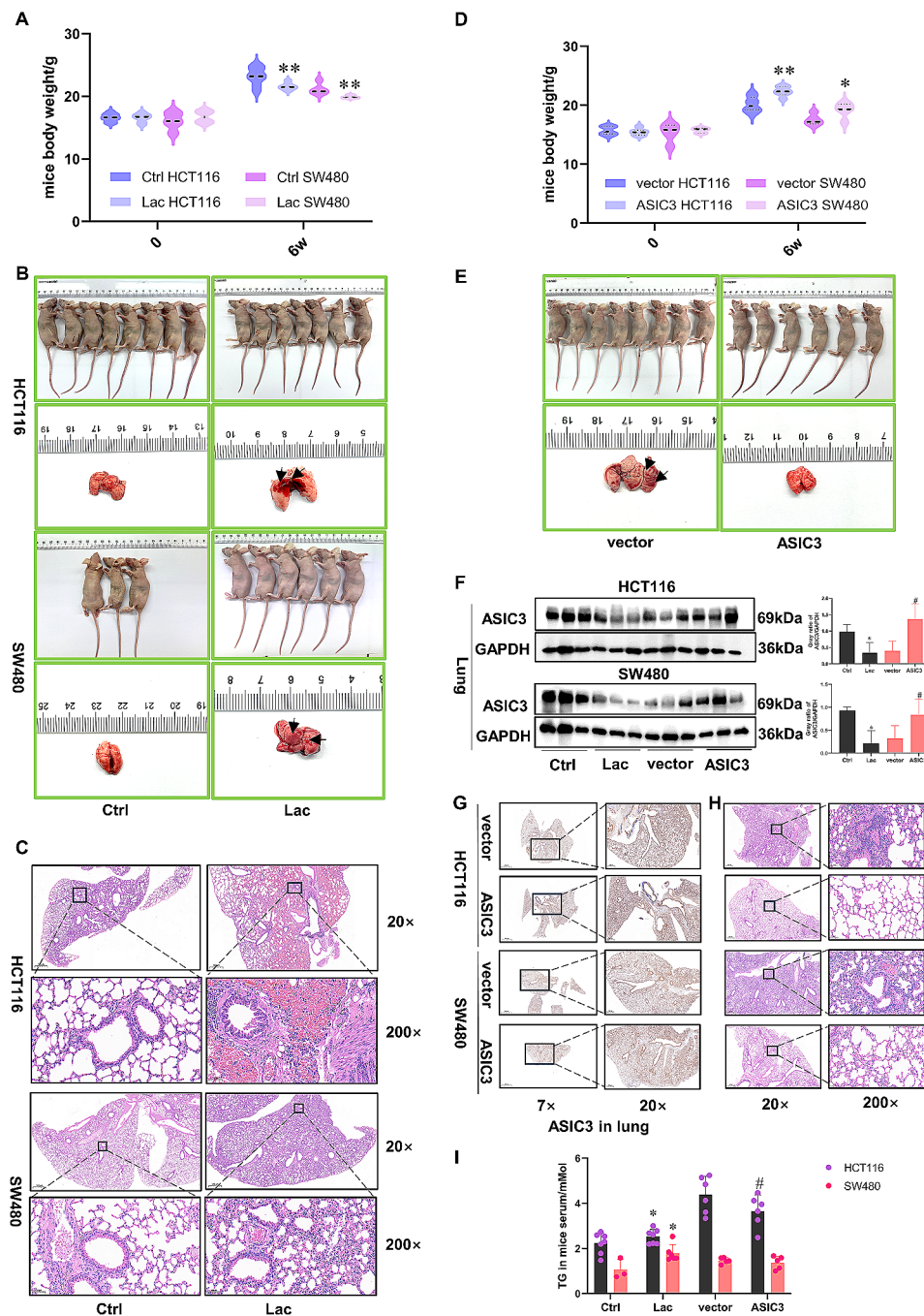
Fig. 8 Overexpression of ASIC3 reverses lactate-induced lung metastasis. **A** The effect of lactate-adapted HCT116 and SW480 cells on nude mice body weight. **B** The effect of lactate-adapted HCT116 and SW480 cells on lung appearance and morphology. **C** The effect of lactate-adapted HCT116 and SW480 cells on lung morphology by HE staining. **D** The changes of nude mice body weight when ASIC3 overexpressed in HCT116 and SW480 cells cultured with lactate. **E** The change of lung morphology when ASIC3 overexpressed in HCT116 cell cultured with lactate. **F** The expression of ASIC3 in lung detected by WB when ASIC3-overexpressed HCT116 and SW480 cells cultured with lactate were injected into mice tail. **G** The expression of ASIC3 in lung detected by IHC when ASIC3-overexpressed HCT116 and SW480 cells cultured with lactate were injected into mice tail. **H** The change of lung morphology observed by HE staining when ASIC3 overexpressed in HCT116 and SW480 cells cultured with lactate. **I** The change of TG in nude mice serum tested by kit when HCT116 and SW480 cells cultured with lactate or overexpressed with ASIC3 were injected into nude mice tail. Error bars represent SD, *or $^{\#}p < 0.05$, **$p < 0.01$

gain in the animals (Fig. 8D), reduced lung hemorrhage, edema, and colorectal cancer metastasis in the lungs(Fig. 8E-H). We also detected the expression of

ASIC3 in the lungs by WB and IHC at the same time, and found that the expression of ASIC3 at metastasis site was negatively correlated with the amount of metastasis,

with higher ASIC3 expression associated with reduced metastasis (Fig. 8F-G). Finally, we detected the content of TG in the animal serum, and found that lactate-cultured HCT116 and SW480 cells could increase the content of TG in serum, while overexpression of ASIC3 decreased TG levels (Fig. 8I), the results of in vivo experiment were consistent with those *in vitro.*

Discussion

Acidosis is considered a chronic form of TME that promotes cell growth and metastasis. Although a large body of literature supports acidosis as a cancer marker or driver, but the core mechanisms by which it affects cancer progression remain unclear, hindering the development of new therapeutic targets and treatments. Here, our research reveals a major, direct, and well-defined molecular signaling pathway that is responsible for acidic TME-induced tumor metastasis. A key and innovative finding of our work is the demonstration that acidic TME can trigger colorectal cancer metastasis by downregulating the ASIC3 sensor. ACC1 and SCD1 are the regulatory targets of ASIC3. The suppression of ASIC3 leads to the activation of *de novo* lipid synthesis, resulting in elevated levels of MUFA that, *in turn*, promote epithelial-mesenchymal transition (EMT) and enhance invasion.

Clinical biopsy revealed variations in lactate content among different tumor tissues, and even acidity in different parts of the same tumor tissue was also different depending on the distance from blood vessels [22]. In this study, we acidified the culture medium using an appropriate concentration of lactate, a glycolysis metabolite [18, 23], and observed that only when exposed to lactate at the correct concentration and duration did colorectal cancer cells exhibit distinct interstitial characteristics, subsequently promoting migration, invasion, and metastasis.

ASICs belong to the degenerin/epithelial sodium channel (DEG/ENaC) superfamily, and are H^+-gated, these ion channels have three states: resting, open, and desensitized [24]. In the human body, there are four main ASIC subtypes: ASIC1, ASIC2, ASIC3 and ASIC4. *They have been linked to various physiological processes such as* myocardial ischemia, memory for learning, inflammation, injury perception and mechanical stimuli [25–27]. While ASIC1 is extensively studied in relation to cancer cells [28], there is limited research on ASIC2 and ASIC3. Although ASIC2 has been reported in colorectal cancer [29], ASIC2 is less sensitive to pH, only when it binds to ASIC1 or ASIC3 to form heteropolymers, can it be more sensitive to pH [30], however, ASIC1 and ASIC3 exhibit higher proton sensitivity, pH at just 7 can activate ASIC3[31∼33]. ASIC1 is desensitized a few seconds after binding to H^+, and even if the pH drops below 7, ASIC1 remains in a persistent desensitized state, which severely limits the signal transmission of ASIC1 in persistent acidosis unless the pH is restored above 7 [31, 34]; unfortunately, the acid environment of colorectal cancer is a chronic continuous process, and only ASIC3 has a plateau activated by long-term acidosis [35]. Interestingly, different from other cancers, in colorectal cancer, lactate has been observed to reduce ASIC3 mRNA and protein expression in a time- and dose-dependent manner, and interference of ASIC3 expression with lentiviruses and shRNA affected acidosis-induced EMT and tumor invasion and metastasis. Additionally, inhibiting ASIC3 currents with amiloride enhances the effects of acidosis on cellular functions.

Scholars have recently provided evidence that tumor acidic microenvironment could in turn influence the metabolism of cancer cells [36∼41]. Studies have shown that cancer cells prefer glutamine metabolism over glucose metabolism when maintained at a pH of 6.5 [39]. Additionally, literature has highlighted significant alterations in fatty acid metabolism in response to ambient acidosis, with fatty acid oxidation (FAO) serving as a primary source of acetyl-CoA to support the TCA cycle [40]. In contrast, the relationship between metabolic preference at acidic pH and local/metastatic invasiveness is only beginning to be explored [40–41]. Thus, new insights into the interaction between acid-driven metabolic preferences and invasive behavior are particularly needed. It was also clearly observed that acidosis can reshape the *de novo* lipid synthesis pathway, increasing the content of unsaturated lipids, especially TG and MUFA, which are the causes of EMT, and ASIC3, located in upstream, can activate and interact with ACC1 and SCD1, key enzymes of *de novo* lipid synthesis pathway, then affects the production of these unsaturated fatty acids, last decrease the ability of acidosis in changing the cell phenotype. To confirm the presence of the ASIC3-ACC1/SCD1 axis, inhibitors of both ACC1 and SCD1 were utilized to restore ASIC3 function, revealing that both inhibitors could counteract ASIC3-mediated acidosis invasion.

Last, our study indicates that ASIC3 is a specific, reliable and significant marker for acidic TME in colorectal cancer. Firstly, unlike other tumors, ASIC3 is down-regulated in colorectal cancer tissues and acidic microenvironment. Secondly, in addition to bioanalysis, a large number of clinical data indicate down-regulated ASIC3 is associated with differentiation, metastasis and staging of colorectal cancer. Animal experiments show that overexpression of ASIC3 can reduce tumor metastasis induced by acidosis. Lastly, given that metabolic reprogramming is a hallmark of cancer, targeting the upstream regulator ASIC3 may lead to improved efficacy in clinical treatment.

Conclusion

A suitable acidic tumor microenvironment can accelerate colorectal cancer invasion and metastasis, and verify for the first time that this effect is accomplished by inhibiting ASIC3. ASIC3 is a biomarker associated with colorectal cancer progression. The mechanism is that ASIC3 can increase the expression of unsaturated fatty acids through interacting with ACC1 and SCD1 in acidic microenvironment, ultimately leading to the induction of EMT. (see graphical abstract).

Supplementary Information

The online version contains supplementary material available at https://doi.org/10.1186/s12964-024-01762-z.

Supplementary Material 1

Supplementary Material 2

Author contributions
W.X.: Conceptualization, Investigation, Writing – original draft. L.F.: Investigation. L.Z.G.: Funding acquisition. Z.L.M: Conceptualization, Funding acquisition, Supervision, Writing – review & editing. .

Data availability
No datasets were generated or analysed during the current study.

Declarations

Ethics approval and consent to participate
This study was conducted in compliance with the principles of the Declaration of Helsinki. Informed consent was obtained from all the subjects. Ethics approval for human subjects was provided by the Ethics Committee of West China Hospital. Ethics approval for animal work was provided by the Animal Ethics Committee of Sichuan University.

Consent for publication
Not applicable.

Competing interests
The authors declare no competing interests.

Author details
[1]Department of Pharmacology, Sichuan University West China School of Basic Medical Sciences & Forensic Medicine, Chengdu 610041, China [2]Department of Pharmacology, Hubei Minzu University Health Science Center, Enshi 445000, China [3]Department of General Surgery, Colorectal Cancer Center, Sichuan University West China Hospital, Chengdu 610041, China

References

1. Harris B, Saleem S, Cook N, Searle E. Targeting hypoxia in solid and haematological malignancies. J Exp Clin Cancer Res. 2022;41:318.
2. Gerweck LE, Seetharaman K. Cellular pH gradient in tumor versus normal tissue: potential exploitation for the treatment of cancer. Cancer Res. 1996;56:1194–8.
3. Swietach P, Boedtkjer E, Pedersen SF. How protons pave the way to aggressive cancers. Nat Rev Cancer. 2023;23(12):825–41.
4. Cortes Franco KD, Brakmann IC, Feoktistova M, Panayotova Dimitrova D, Gründer S, Tian Y. Aggressive migration in acidic pH of a glioblastoma cancer stem cell line in vitro is independent of ASIC and K(ca)3.1 ion channels, but involves phosphoinositide 3-kinase. Pfugers Arch. 2023;475:405–16.
5. Cremer J, Brohée L, Dupont L, Lefevre C, Peiffer R, Saarinen AM, et al. Acidosis-induced regulation of adipocyte G0S2 promotes crosstalk between adipocytes and breast cancer cells as well as tumor progression. Cancer Lett. 2023;569:216306.
6. Pujals M, Mayans C, Bellio C, Méndez O, Greco E, Fasani R, et al. RAGE/SNAIL1 signaling drives epithelial-mesenchymal plasticity in metastatic triple-negative breast cancer. Oncogene. 2023;42(35):2610–28.
7. Clusmann J, Franco KC, Suarez DAC, Katona I, Minguez MG, Boersch N, et al. Acidosis induces RIPK1-dependent death of glioblastoma stem cells via acid-sensing ion channel 1a. Cell Death Dis. 2022;13:702.
8. Neri D, Supuran CT. Interfering with pH regulation in tumours as a therapeutic strategy. Nat Rev Drug Discov. 2011;10:767e77.
9. Pillai S, Mahmud I, Mahar R, Griffith C, Langsen M, Nguyen J, et al. Lipogenesis mediated by OGR1 regulates metabolic adaptation to acid stress in cancer cells via autophagy. Cell Rep. 2022;39(6):110796.
10. Knopf P, Stowbur D, Hoffmann SHL, Hermann N, Maurer A, Bucher V, et al. Acidosis-mediated increase in IFN-γ-induced PD-L1 expression on cancer cells as an immune escape mechanism in solid tumors. Mol Cancer. 2023;22(1):207.
11. Imenez Silva PH, Camara NO, Wagner CA. Role of proton-activated G protein-coupled receptors in pathophysiology. Am J Physiol Cell Physiol. 2022;323:C400–14.
12. Walenta S, Chau TV, Schroeder T, Lehr HA, Kunz-Schughart LA, Fuerst A, et al. Metabolic classification of human rectal adenocarcinomas: a novel guideline for clinical oncologists? J Cancer Res Clin Oncol. 2003;129(6):321–6.
13. Tian Y, Bresenitz P, Reska A, El Moussaoui L, Beier CP, Gründer S. Glioblastoma cancer stem cell lines express functional acid-sensing ion channels ASIC1a and ASIC3. Sci Rep. 2017;7(1):13674.
14. Wu Y, Gao B, Xiong QJ, Wang YC, Huang DK, Wu WN. Acid-sensing ion channels contribute to the effect of extracellular acidosis on proliferation and migration of A549 cells. Tumour Biol. 2017;39(6):1010428317705750.
15. Qian HY, Zhou F, Wu R, Cao XJ, Zhu T, Yuan HD, et al. Metformin attenuates Bone Cancer Pain by reducing TRPV1 and ASIC3 expression. Front Pharmacol. 2021;12:713944.
16. Zhu S, Zhou HY, Deng SC, Deng SJ, He C, Li X, et al. ASIC1 and ASIC3 contribute to acidity-induced EMT of pancreatic cancer through activating ca(2+)/RhoA pathway. Cell Death Dis. 2017;8(5):e2806.
17. Ding M, Zhang S, Guo Y, Yao J, Shen Q, Huang M, et al. Tumor Microenvironment Acidity triggers lipid Accumulation in Liver Cancer via SCD1 activation. Mol Cancer Res. 2022;20(5):810–22.
18. Liu W, Wang Y, Bozi LHM, Fischer PD, Jedrychowski MP, Xiao H, et al. Lactate regulates cell cycle by remodelling the anaphase promoting complex. Nature. 2023;616(7958):790–7.
19. Wu T, Wan J, Qu X, Xia K, Wang F, Zhang Z, et al. Nodal promotes colorectal cancer survival and metastasis through regulating SCD1-mediated ferroptosis resistance. Cell Death Dis. 2023;14(3):229.
20. She K, Fang S, Du W, Fan X, He J, Pan H, et al. SCD1 is required for EGFR-targeting cancer therapy of lung cancer via re-activation of EGFR/PI3K/AKT signals. Cancer Cell Int. 2019;19:103.
21. Ran H, Zhu Y, Deng R, Zhang Q, Liu X, Feng M, et al. Stearoyl-CoA desaturase-1 promotes colorectal cancer metastasis in response to glucose by suppressing PTEN [J]. J Exp Clin Cancer Res. 2018;37(1):54.
22. Boedtkjer E, Pedersen SF. The acidic Tumor Microenvironment as a driver of Cancer. Annu Rev Physiol. 2020;82:103–26.
23. Zhao Y, Li M, Yao X, Fei Y, Lin Z, Li Z, et al. HCAR1/MCT1 regulates Tumor Ferroptosis through the lactate-mediated AMPK-SCD1 activity and its therapeutic implications. Cell Rep. 2020;33(10):108487.
24. YOSHIOKA YODERN. Gating mechanisms of acid-sensing ion channels. Nature. 2018;555(7696):397–401.

25. Hung CH, Chin Y, Fong YO, Lee CH, Han DS, Lin JH, et al. Acidosis-related pain and its receptors as targets for chronic pain. Pharmacol Ther. 2023;247:108444.
26. Zhang L, Zheng L, Yang X, Yao S, Wang H, An J, et al. Pathology and physiology of acidsensitive ion channels in the digestive system. Int J Mol Med. 2022;50(1):94.
27. Wu WL, Cheng CF, Sun WH, Wong CW, Chen CC. Targeting ASIC3 for pain, anxiety, and insulin resistance. Pharmacol Ther. 2012;134(2):127–38.
28. Wang Y, Zhou H, Sun Y, Huang Y. Acid-sensing ion channel 1: potential therapeutic target for tumor. Biomed Pharmacother. 2022;155:113835.
29. Zhou ZH, Song JW, Li W, Liu X, Cao L, Wan LM, et al. The acid-sensing ion channel, ASIC2, promotes invasion and metastasis of colorectal cancer under acidosis by activating the calcineurin/NFAT1 axis. J Exp Clin Cancer Res. 2017;36(1):130.
30. Gründer S, Vanek J, Pissas KP. Acid-sensing ion channels and downstream signalling in cancer cells: is there a mechanistic link? Pflugers Arch. 2024;476(4):659–72.
31. Babini E, Paukert M, Geisler HS, Gründer S. Alternative splicing and interaction with di- and polyvalent cations control the dynamic range of acid-sensing ion channel 1 (ASIC1). J Biol Chem. 2002;277:41597–603.
32. Chen CC, England S, Akopian AN, Wood JN. A sensory neuron-specific, proton-gated ion channel. Proc Natl Acad Sci USA. 1998;95:10240–5.
33. Joeres N, Augustinowski K, Neuhof A, Assmann M, Gründer S. Functional and pharmacological characterization of two different ASIC1a/2a heteromers reveals their sensitivity to the spider toxin PcTx1. Sci Rep. 2016;6:27647.
34. Gründer S, Pusch M. Biophysical properties of acid-sensing ion channels (ASICs). Neuropharmacology. 2015;94:9–18.
35. Yagi J, Wenk HN, Naves LA, McCleskey EW. Sustained currents through ASIC3 ion channels at the modest pH changes that occur during myocardial ischemia. Circ Res. 2006;99:501–9.
36. Khacho M, Tarabay M, Patten D, Khacho P, MacLaurin JG, Guadagno J, et al. Acidosis overrides oxygen deprivation to maintain mitochondrial function and cell survival. Nat Commun. 2014;5:3550.
37. Nadtochiy SM, Schafer X, Fu D, Nehrke K, Munger J, Brookes PS. Acidic pH is a metabolic switch for 2-hydroxyglutarate generation and signaling. J Biol Chem. 2016;291:20188–97.
38. Kondo A, Yamamoto S, Nakaki R, Shimamura T, Hamakubo T, Sakai J, et al. Extracellular acidic pH activates the sterol regulatory element binding protein 2 to promote tumor progression. Cell Rep. 2017;18:2228–42.
39. Corbet C, Draoui N, Polet F, Pinto A, Drozak X, Riant O, et al. The SIRT1/HIF2alpha axis drives reductive glutamine metabolism under chronic acidosis and alters tumor response to therapy. Cancer Res. 2014;74:5507–19.
40. Corbet C, Pinto A, Martherus R, Santiago de Jesus JP, Polet F, Feron O. Acidosis drives the reprogramming of fatty acid metabolism in cancer cells through changes in mitochondrial and histone acetylation. Cell Metab. 2016;24:311–23.
41. Wojtkowiak JW, Rothberg JM, Kumar V, Schramm KJ, Haller E, Proemsey JB, et al. Chronic autophagy is a cellular adaptation to tumor acidic pH microenvironments. Cancer Res. 2012;72:3938–47.

Publisher's Note